Original Research

Patient-specific molecular response dynamics can predict the possibility of relapse during the second treatment-free remission attempt in chronic myelogenous leukemia

Eunjung Kim [a,1,*]; Eo-Jin Hwang [b]; Junghye Lee [c];
Dae-Young Kim [d]; Jae-Young Kim [e,1,*];
Dong-Wook Kim [d,b,1,*]

[a] Natural Product Informatics Research Center, Korea Institute of Science and Technology, Gangneung, South Korea
[b] Leukemia Omics Research Institute, Eulji University Uijeongbu Campus, Uijeongbu, South Korea
[c] Department of Industrial Engineering, Ulsan National Institute of Science and Technology, Ulsan, South Korea
[d] Department of Hematology, Hematology center, Uijeongbu Eulji Medical Center, Eulji University, Uijeongbu, South Korea
[e] Graduate School of Analytical Science and Technology (GRAST), Chungnam National University, Daejeon, South Korea

Abstract

In chronic myelogenous leukemia (CML), treatment-free remission (TFR) is defined as maintaining a major molecular response (MMR) without a tyrosine kinase inhibitor (TKI), such as imatinib (IM). Several studies have investigated the safety of the first TFR (TFR_1) attempt and suggested recommendation guidelines for such an attempt. However, the plausibility and predictive factors for a second TFR (TFR_2) have yet to be reported.

The present study included 21 patients in chronic myeloid leukemia who participated in twice repeated treatment stop attempts. We develop a mathematical model to analyze and explain the outcomes of TFR_2. Our mathematical model framework can explain patient-specific molecular response dynamics. Fitting the model to longitudinal *BCR-ABL1* transcripts from the patients generated patient-specific parameters. Binary tree decision analyses of the model parameters suggested a model based predictive binary classification factor that separated patients into low- and high-risk groups of TFR_2 attempts with an overall accuracy of 76.2% (sensitivity of 81.1% and specificity of 69.9%). The low-risk group maintained a median TFR_2 of 28.2 months, while the high-risk group relapsed at a median time of 3.25 months. Further, our model predicted a patient-specific optimal IM treatment duration before the second IM stop that could achieve the desired TFR_2 (e.g., 5 years).

Introduction

Chronic myelogenous leukemia (CML) is a myeloproliferative disorder that results from the translocation of chromosomes 9 and 22 which leads to the expression of the oncogenic *BCR-ABL1* fusion tyrosine kinase and the clonal expansion of transformed multipotent hematopoietic stem cells [1,2].

The current standard of care for CML is oral administration of tyrosine kinase inhibitors (TKIs) targeting oncogenic ABL tyrosine kinase activity. Imatinib (IM), the first Food and Drug Administration (FDA)-approved TKI for CML treatment, has dramatically improved the outcomes of patients with CML [3–5].

After five years of IM therapy, approximately 50% of chronic-phase patients can achieve a deep molecular response (DMR): A molecular response greater than a 4-log reduction (MR [4]) is defined as a *BCR-ABL1/ABL1* level less than or equal to 0.01% (*BCR-ABL1/ABL1* ≤ 0.01%). A molecular response greater than a 4.5-log reduction (MR [4,5]) is defined as a *BCR-ABL1/ABL1* level less than or equal to 0.0032% (*BCR-ABL1/ABL1* ≤ 0.0032%).[6–8] However, due to their side effects, toxicities, and high treatment costs, TKIs need to be safely discontinued [9,10]. Several studies have shown that patients who achieve a DMR (MR [4,5]) can discontinue TKIs, and the achievement of long-term treatment-free remission (TFR) is an important clinical goal after TKI cessation [11–15].

To support the clinical decision for safe TKI discontinuation, it is crucial to identify factors that can predict the risk of molecular relapse after therapy cessation. A multicenter stop imatinib (STIM) study showed that the duration of IM therapy before the first treatment stop is associated with molecular relapse after the cessation [12]. In another study, Takahashi et al. [16] showed that the duration of a major molecular response (MMR) (3-log reduction in the *BCR-ABL1/ABL1* transcript ratio, *BCR-ABL1/ABL1* $\leq$ 0.1%) is strongly associated with molecular relapse-free five-year survival rate following the first IM discontinuation. In our previous work, we observed that treatment duration and the occurrence of IM withdrawal syndrome are associated with a lower risk of molecular relapse in TFR_1 attempts [11,17]. It should be noted that IM withdrawal syndrome consists of musculoskeletal pain that resembles Polymyalgia Rheumatica after tyrosine kinase inhibitor therapy cessation [18]. Daher-Reyes et al. [19] reported that the doubling time of the *BCR-ABL1* transcript within the first six months after IM discontinuation could be a predictive marker for a successful TFR_1 attempt. The European LeukemiaNet recently suggested guidelines for safe TKI discontinuation, including a duration of DMR > 2 years and TKI therapy duration > 5 years [20]. It has also been reported that early molecular response dynamics assessed by the *BCR-ABL1* halving time after TKI treatment could be a predictive factor for TFR_1[21]. A recent study raised the possibility of a potential molecular marker that could predict TFR. Shen et al. reported that folate receptor 3 (FOLR3) was highly expressed in some non-relapsed patients whereas it was not expressed in any relapsed patients. Further, the presence of a single nucleotide polymorphism (SNP) in this gene was associated with the risk of relapse after TKI cessation [22]. Patients who experience molecular relapse (*BCR-ABL1/ABL1* increased to 0.1%) after the first IM discontinuation can receive a second round of TKI treatment. Patients who achieve MMR again are eligible for a second TKI stop attempt. However, predictive markers that could support a clinical decision for the second TKI discontinuation are currently lacking.

Several mathematical models have been developed in attempts to understand the first principles of leukemic cell dynamics upon the administration of IM therapy. Some models that are combined with clinical data involving one-time IM cessation have been used to predict the prognosis of treatment discontinuation. A mathematical model explaining the biphasic kinetics of leukemic cell decline upon IM therapy has suggested that the limited ability of IM to eradicate leukemic stem cells is associated with IM resistance [23]. In another study, Tang et al. [24] performed statistical analyzes of STIM study data and developed a mathematical model to provide insights into the two different outcomes (cure vs. no-cure scenario) of the trial. An agent-based mathematical model that describes hematopoietic stem cell organization has suggested that the number of residual leukemic stem cells at the time of IM stop is a prognostic factor of IM discontinuation [25]. However, none of these models has been applied to a second TFR attempt (TFR_2).

In this study, we describe the molecular response of chronic phase CML patients who underwent both the first and second TFR attempt by utilizing a mathematical modeling approach. Specifically, we developed a mathematical model that could simulate the dynamics of leukemic stem cells, leukemic progenitor cells, differentiated leukemic cells, and *BCR-ABL1* levels during two repeat cycles of on and off IM therapy. The model was calibrated and validated with longitudinal *BCR-ABL1* measurements from individual patients. Based on patient-specific model parameters that control *BCR-ABL1* dynamics, we suggest model-based predictive factors for the risk of relapse during TFR_2 that could be used to support the clinical decision for a future second TFR attempt.

Study patients

This study involved a cohort of 21 chronic-phase patients treated with frontline IM therapy who relapsed during the first TFR attempt and re-

achieved MMR upon the reapplication of IM. These patients then underwent a second TFR attempt. The patients fulfilled the criteria for safe treatment discontinuation [20]. The characteristics of these patients are summarized in Table 1. The median age was 40 years old (range, 18–63 years old). Before the first discontinuation, the median duration of the initial IM treatment was 68 months (range, 38–136 months). The period of a sustained molecular response (MR [5]) (*BCR-ABL1/ABL1* $\leq$ 0.001%) was 32.9 months (range, 24–103 months). During IM discontinuation, the *BCR-ABL1* transcript level was analyzed using a quantitative reverse transcriptase polymerase chain reaction (qRT-PCR) assay with the following monitoring schedule: every 1-2 months for the first six months, every 2-3 months from the first six months to 12 months, and every three months thereafter. All 21 patients relapsed within a median follow-up period of 4 months (range: 2–21 months) in the TFR_1 attempt. Upon the initial identification of a loss of MMR (MMR: *BCR-ABL1/ABL1* $\leq$ 0.1%), a consecutive second assessment was performed within four weeks. In cases of repeated MMR loss (molecular relapse), IM treatment was reintroduced, thus resulting in a re-achievement of MR [5] at a median of 5.6 months (range, 1.8–12.1 months). After sustaining MR [5] for a median of 31 months (range, 14–44 months) of IM therapy, IM treatment was discontinued again. In this cohort, 16 patients experienced relapse within a median period of 4.8 months (range: 1.8–31 months). The remaining five patients maintained TFR_2 with a median duration of 33 months (range, 23–47 months). This study was approved by the institutional review board and was conducted according to the Declaration of Helsinki.

Materials and methods

Mathematical model

We developed a mathematical model that describes CML cell dynamics based on the biology of the hematopoietic differentiation hierarchy system [26,27]. Morrison et al. proposed the hierarchy of the hematopoietic system, which is composed of stem cells, progenitor cells, and differentiated cells [26,27]. Like normal hematopoiesis, leukemogenesis is also known to be hierarchically organized [28]. Based on these biological data, we developed a model composed of three cell types: leukemic stem cells, leukemic progenitor cells, and leukemic differentiated cells. It should be noted that we did not consider the interaction between normal hematopoietic cells and leukemic cells since leukemic cells can outcompete healthy cells and already escape homeostatic control by normal cells [29–31]. Leukemic cells can modify or hijack their microenvironments to promote their expansion [32,33]. However, we assume that all leukemic cells had already acquired these fitness advantage over normal cells at the point of diagnosis (∼100 international scale corresponding to 10^{12} cells), [34] and therefore we do not consider normal cells' influence on leukemic cells in this study.

In the model, the abundance of cells is denoted by *S* (leukemic stem cells), *P* (leukemic progenitor cells), and *D* (leukemic differentiated cells). The *S* population divides at a rate of r_S per day, dies at a rate of δ_S, and produces a *P* cell population at a rate of φ. The *P* cell population divides at a rate of r_P and dies at a rate of δ_P. Since research has shown that the expansion of the *S* cell population can be modulated by competition, [31,35] we assumed density-dependent growth of the *S* cell population (i.e., growth modulated by the *S* and *P* cell populations residing in the same microenvironment) [35,36]. This density dependency has also been used by other mathematical modeling studies [23,24,37]. The *P* cell population generates the *D* cell population at a rate of ξ. The natural death rate for the *D* cell population is denoted by δ_D.

IM treatment can reduce the expansion of leukemic progenitor cells and differentiated cells [23]. Studies with CML patients who underwent IM therapy showed that IM treatment also potentially inhibits the expansion of leukemic stem cells [35,37,38]. Based on the biological and clinical data, our model assumes that IM therapy can inhibit the expansion of the *S* (increased cell death rate, δ_S) and *P* (increased cell death rate δ_P) cell populations

Table 1

Patient characteristics.

Parameters	Patients ($N = 21$)
Age (yr), median (range)	40 (18-63)
1st stop	
IM therapy duration (mo), median (range)	68 (38-136)
Period of MR[5] before IM cessation (mo), median (range)	32.9 (24-103)
Duration of TFR$_1$ (mo), median (range)	4 (2-21)
2nd stop	
IM therapy duration (mo), median (range)	31 (14-44)
Period of MR[5] before IM cessation (mo), median (range)	5.6 (1.8-12.1)
Duration of TFR$_2$, relapsed, (mo), median(range)	4.8 (1.8-31) ($n = 16$)
Duration of TFR$_2$ (mo), median (range)	33 (23-47) ($N = 5$)

Abbreviation: IM, imatinib, MR[5], ($BCR\text{-}ABL1/ABL1 \leq 0.001\%$), yr: year, mo: months.

and decrease the differentiation from the P to D cell populations (decreased differentiation rate from P to D, ξ by a factor (F)). We provide the following rationale for why IM can inhibit leukemic stem: The first reason is the biphasic decline in $BCR\text{-}ABL1/ABL1$ transcripts in patients treated with an imatinib (IM) therapy. The initial sharp decline is caused by the eradication of proliferating leukemic cells, and the second decline is attributed to leukemic stem cell death or the inhibition of differentiation [23,37,39–41]. The second reason is that mathematical analyzes of the IRIS (a phase 3 international randomized study of interferon and ST1571) [38] revealed that an IM therapy prevents the proliferation of leukemic stem cells, thus causing the leukemic stem cell compartment to die out. Otherwise, rapid relapse during long-term IM therapy is inevitable (∼7-8% relapse at the 5th year of IM therapy; ∼50% relapse at the 6th year of IM therapy).

Based on the model assumptions, we develop the following mathematical model.

$$\frac{dS}{dt} = \left(\frac{r_S}{f(S, P)} - \delta_S \right)S,$$

$$\frac{dP}{dt} = \varphi S + (r_P - \delta_P)P,$$

$$\frac{dD}{dt} = \psi P - \delta_D D,$$

where

$$\delta_S = \begin{pmatrix} 0, \text{ if IM off} \\ \delta_S, \text{ if IM on} \end{pmatrix}, \quad \delta_P = \begin{pmatrix} 0, \text{ if IM off} \\ \delta_P, \text{ if IM on} \end{pmatrix}, \psi = \begin{pmatrix} \xi, \text{ if IM off} \\ \xi/_F, \text{ if IM on} \end{pmatrix}, \text{ where }$$

$F \geq 1$ indicates the reduction rate by the treatment. In the model, $f(S, P) = S + P$, where $S + P > 0$.

As this system of nonlinear differential equations cannot be solved in closed form, we numerically solved the equations utilizing an ODE solver (ode15s) in MATLAB (MathWorks, Boston, MA, USA).

Parameterization

The model parameter identification and estimation process were performed by applying a numerical sensitivity analysis, a structure correlation analysis, and numerical optimization (a more detailed explanation of this process is presented in the supplementary method). Based on our sensitivity analysis (Fig. S1A) and structure correlation analysis (Fig. S1B), the parameter r_S was determined to be the least sensitive and mostly correlated parameter, and so it was set to be a fixed value for all patients ($r_S =0.001$, comparable to the previous estimation by other groups) [24,37].

To compare patient $BCR\text{-}ABL1$ to $ABL1$ ratio data, we calculated the model predicted $BCR\text{-}ABL1$ to $ABL1$ ratio as $D/(2N + D) \times 100\%$, where N represents the number of healthy differentiated cells, and D indicates

the mathematical model-predicted leukemic differentiated cell population. A healthy cell has two copies of $ABL1$, while a leukemic cell has one copy of ABL1 and one copy of $BCR\text{-}ABL1$. qRT-PCR assays are typically performed on peripheral blood and differentiated cells account for most of the cells analyzed by the assay. The $BCR\text{-}ABL1/ABL1$ ratio in blood is known to correlate with the cytogenic assessment of leukemic cells in bone marrow, and it is shown to be reliable for monitoring tumor burden [6,42–44]. This calculation method has been used in several previous studies [23,24,37]. The number of white blood cells was used to set a value for N (Table S1). The initial D cell population (D_0) in the model could be directly derived from the initial $BCR\text{-}ABL1/ABL1$ level for each patient by solving the linear equation $D_0/(2N + D_0) \times 100 = B_0$ for D_0, where N is the number of normal cells (Table S1) and B_0 is the $BCR\text{-}ABL1/ABL1$ data at the beginning of therapy.

The remaining parameters were estimated by comparing the individual patient longitudinal change in $BCR\text{-}ABL1$ to $ABL1$ ratio with the model-predicted $BCR\text{-}ABL1$ to $ABL1$ ratio ($M(H; t_i) = D(H; t_i)/(2N + D(H; t_i))$, where H is the model parameter set, t_i is time, D is differentiated cell population, and N is the number of healthy differentiated cells). Next, for each patient, we separated the $BCR\text{-}ABL1/ABL1$ data points into two sets: the training set and the testing set. The training set is composed of $BCR\text{-}ABL1$ data points collected from the start of treatment to the first relapse, while the testing set is composed of the data points collected from first relapse to the end of data collection. We used the training set data to estimate patient-specific model parameters that minimized the difference between the patient qRT-PCR data and the model-predicted $BCR\text{-}ABL1$ to $ABL1$ ratio. The accuracy of the model parameterization was assessed on the testing set. Linear regression of simulated versus measured $BCR\text{-}ABL1/ABL1$ ratios yielded an R^2 of 0.66 (Fig. S1C).

We next evaluated the impact of density-dependent growth control of the S cell population on model performance. The model without density-dependent feedback produced a lower R^2 value (R^2 of 0.54) than the original model (R^2 of 0.66) (Fig. S2). We therefore conclude that the density-dependent term helps accurately describe the patient data.

Statistical analysis

The probability of TFR was plotted using the Kaplan-Meier method and compared using the log-rank test. We utilized binary tree analysis in MATLAB [45,46] to identify predictors and cutoffs that could be used to separate patients into low-risk and high-risk TFR$_2$ attempt groups. This statistical method is often used to study relationships between a response variable (e.g., TFR$_2$ in our study) and predictor variables (e.g., predictive markers in our study). This method can predict a response by recursively partitioning data into two subgroups based on the predictor values.
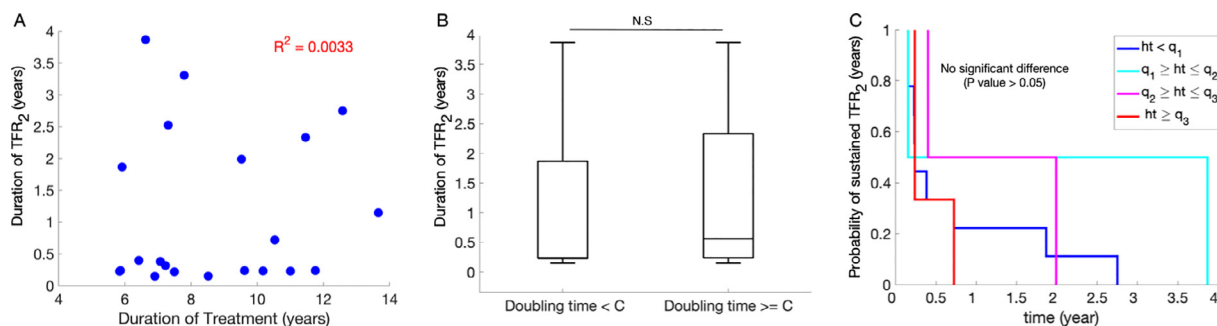
Fig. 1. Existing predictive factors for TFR$_1$ fail to predict TFR$_2$. A: No linear correlation between the duration of IM therapy and the duration of TFR$_2$. B: Duration of TFR$_2$ and doubling time criteria for TFR$_1$ separation (C = 12.71 days).[19] N.S: not significant (p value > 0.05, Student t-test). C: Halving time (ht) and probability of a sustained TFR$_2$. The probabilities were not significantly different among the four patient groups separated by the previously identified halving times of q$_1$ (=9.35 days), q$_2$ (=13.95 days), and q$_3$ (=21.85).[21]

Results

Patient-specific molecular response to IM therapy and discontinuation

We observed highly differential TFR durations between the patients in our study (Table 1 and Fig. S3). During the TFR$_1$ attempt, four patients maintained TFR$_1$ for longer than six months, while others relapsed within 2–6 months. In contrast to the TFR$_1$ attempt, patients tended to maintain a longer TFR in the second IM discontinuation attempt. Approximately half ($n = 9$) of the patients maintained TFR$_2$ for longer than six months. Motivated by these diverse interindividual BCR-ABL1 kinetic responses, we aimed to identify predictive markers for relapse during the second TFR attempt.

Predictive factors for TFR$_1$ are less likely predictive of TFR$_2$

Predictive factors for TFR$_1$ have already been reported in previous studies [11,12,17,19–21]. We evaluated the ability of these predictive factors to determine the risk of relapse during the second treatment stop attempt (TFR$_2$). In our study, the duration of IM therapy was not correlated with the duration of TFR$_2$ (Fig. 1A, R^2=0.003). Doubling time within the six months after treatment discontinuation, a known predictive factor for TFR$_1$, was not found to be an effective predictor for TFR$_2$. Further, the duration of TFR$_2$ separated by the doubling time was not significantly different (Fig. 1B, Student's t-test, p-value > 0.05). Last, the probabilities of a sustained TFR$_2$ in the four different groups divided by the halving time were not significantly different (Fig. 1C, log-rank test, p-value > 0.05). The results of these analyzes highlight the need to identify factors for predicting the probability of a sustained TFR$_2$ or the risk of relapse during the second treatment stop.

The mathematical model simulates patient-specific molecular response dynamics

To develop predictive factors specifically for the TFR$_2$ attempt, there is a need for a method to predict BCR-ABL1/ABL1 dynamics during on and off IM therapy. The dynamics of the BCR-ABL1/ABL1 transcript levels represent changes in differentiated leukemic cells in response to on and off therapy. We developed a personalized mathematical model that could explain the patient-specific leukemic cell dynamics governing temporal BCR-ABL1/ABL1 changes during on and off therapy. To elaborate, our model is an ordinary differential equation model that can explain the temporal evolution of cell populations based on the architecture of hematopoietic differentiation. The model describes the dynamic behaviors of three leukemic cell types: leukemic stem cells (S), leukemic progenitor cells (P), and leukemic differentiated cells (D) (Fig. 2). A detailed description is provided in the mathematical model section (materials and methods).

Fitting the model to a training set provided patient-specific model parameters that minimized the least squared error between the model-predicted BCR-ABL1/ABL1 levels and the patient BCR-ABL1/ABL1 levels (a more detailed explanation is provided in the parameterization section in the supplementary methods). The accuracy of this model was assessed by comparing the model-predicted BCR-ABL1/ABL1 levels with patient data from the testing set (Figs. 3A and S4, blue lines). The L$_2$ norm error

$$\left(\|\text{error}\|_2 = \sqrt{\sum_{i=1}^{n} \left(Model(t_i) - Data(t_i) \right)^2}, \ t_i: \text{testing set time points} \right)$$ values

for each patient are presented.

The fitted model predicted the underlying dynamics of the S, P, and D cell populations in each patient. Fig. 3B–D show the dynamics of the S, P, and D cell populations in a representative patient who relapsed during both the first and the second IM discontinuation attempts. As can be seen in the figure, the S cell population in this patient decreased with IM therapy, but it then slightly increased during IM removal. The rate of the decrease in the P cell population during IM therapy was higher than that in the S cell population. Further, the P cell population increased during IM cessation. The D cell population dynamics were similar to those of the P cell population.

### Mathematical model-based predictive binary classifier for TFR$_2$

By employing patient-specific model parameters governing the dynamics of the S, P, and D cell populations for each patient, we attempted to identify predictive factors for the risk of relapse during the second treatment free remission attempt (TFR$_2$). It should be noted that we assumed that a low risk indicates a longer period of TFR$_2$. A binary tree analysis identified both the most significant predictor (δ_S/r_P) and the cutoff that separates a high risk from a low risk of relapse during TFR$_2$ (Fig. S5A, B, a more detailed explanation in the supplementary method). Among the 21 patients considered, 13 had δ_S/r_P values under the cutoff for δ_S/r_P, while the remaining 8 had values exceeding the cutoff. Patients with a high δ_S/r_P were classified into the low-risk relapse group ($n = 8$), while those with a low δ_S/r_P were classified into the high-risk relapse group ($n = 13$) for the TFR$_2$ attempt. To assess the accuracy of this predictive factor, receiver operating characteristic (ROC) curve analysis was performed (supplementary methods) [47]. An ROC curve is a graph of a classifier's sensitivity versus its false-positive rate (1-specificity). The area under the ROC curve (AUC), a summary measure was 0.744 (AUC = 1 indicating perfect classification ability and AUC < 0.5 indicating no classification ability). The overall accuracy of this classifier was found to be 76.2% (95% confidence interval CI: (66.1%, 86.3%)), with a
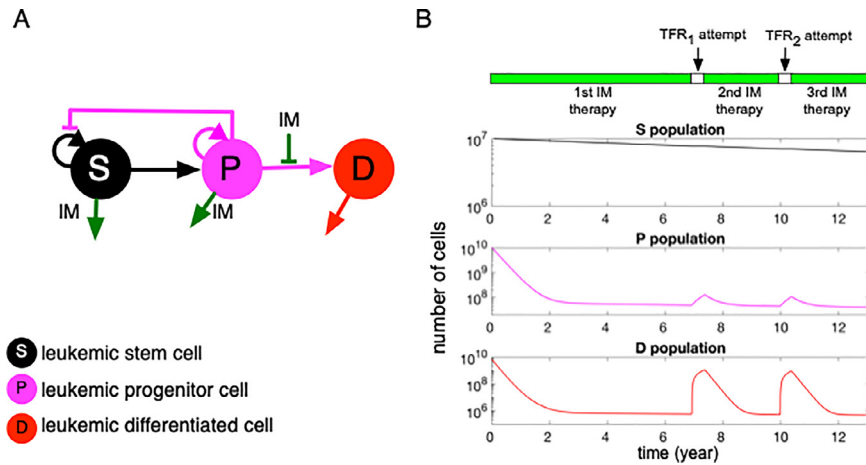
Fig. 2. Mathematical model development. A: A diagram showing the mathematical model. *S*: Leukemic stem cell population; *P*: Leukemic progenitor cell population; *D*: Leukemic differentiated cell population; green line: the effect of IM (imatinib) on each cell compartment: increasing cell death rates of the *P* and *S* cell populations and inhibiting the differentiation from *P* cells to *D* cells. B: Model-predicted dynamics of the *S, P,* and *D* populations in one representative patient. Green bar: treatment on, white bar: treatment off.
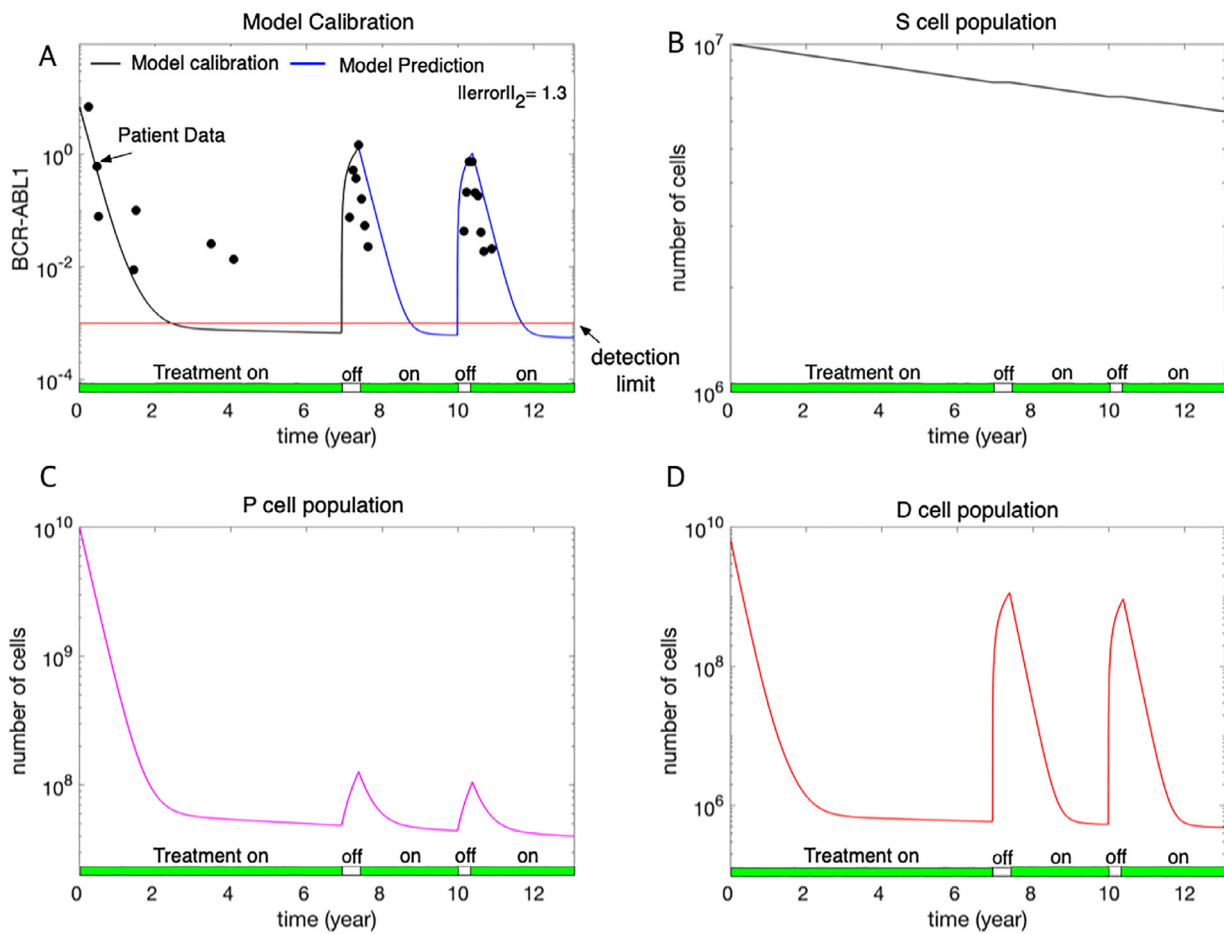
Fig. 3. A: Model calibration. Calibration of the mathematical model using representative *BCR-ABL1/ABL1* data (black dots) from a patient who relapsed during both TFR$_1$ and TFR$_2$ attempts. (Fig. S4 presents the model calibration for all patients). Black solid line: average over model simulations from treatment start to the first relapse (training set) using parameter sets that lead to equally good fit; blue line: average over model simulations from the first relapse to the time end of record using parameter sets that lead to equally good fit; the L$_2$ norm error ($\|\text{error}\|_2 = \sqrt{\sum_{i=1}^{n} (Model(t_i) - Data(t_i))^2}$, t_i: testing set time points) is reported. B-D: Model-predicted changes in the *S* (leukemic stem cell), *P* (leukemic progenitor cell), and *D* (leukemic differentiated cell) populations. The green bar indicates the therapy on period; and the white bar indicates the therapy off period.
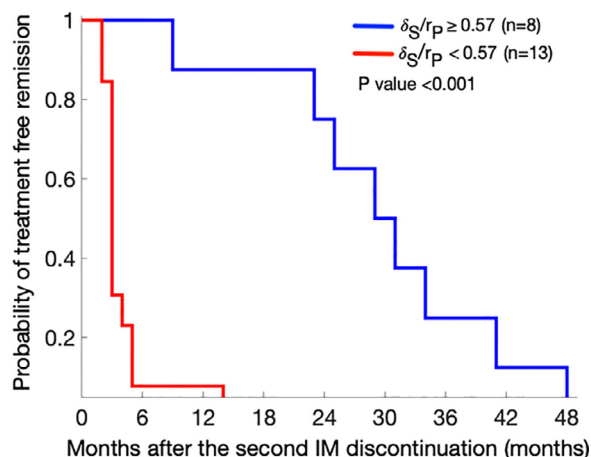
Fig. 4. Kaplan-Meier curves of TFR$_2$ in two sub cohorts classified by the classifier $\frac{\delta_S}{r_P}$. The log-rank test was performed (p-value < 0.001).

sensitivity of 81.8% (95% CI: (62.8%, 99.9%)) and a specificity of 66.9% (95% CI: (46.2%, 87.7%)).

We next compared the TFR$_2$ probabilities between the high-risk group and the low-risk group. Fig. 4 presents the results of the log-rank test and the Kaplan-Meier curves of these two patient groups (the high-risk group made up of the 13 patients with a low δ_S/r_P and the low-risk group made up of the 8 patients with a high δ_S/r_P). The average TFR$_2$ duration of the high-risk group was four months (range: 2–14 months), while that of the low-risk group was 30 months (range: 9–48 months). The probability of TFR$_2$ in the low-risk group was significantly different from that in the high-risk group (log-rank test, p-value < 0.001). Taken together, the results indicate that model-derived parameters successfully differentiated the high-risk TFR$_2$ group from the low-risk TFR$_2$ group.

Optimal IM therapy duration for 5-year TFR$_2$

We predicted the optimal treatment duration for the 2nd IM treatment (i.e., the duration that could achieve the desired duration of TFR$_2$) in the low-risk group using the Monte Carlo Method (a detailed explanation is provided in the supplementary methods). We solely considered the low-risk group because the high-risk group was predicted to relapse quickly during the TFR$_2$ attempt, even with a sufficient IM therapy duration (> 10 years); thus, treatment cessation may not be a safe option for patients in the high-risk group. For the low-risk group ($n = 8$), we set the desired duration of TFR$_2$ to 5 years and predicted the IM therapy duration to achieve this desired duration (the supplementary methods provide a more detailed explanation). Fig. 5 shows the individual patient *BCR-ABL1/ABL1* dynamics with the optimal duration of IM therapy. Five patients required less than three years of IM therapy (range: 1.5–2.4 years), while the remaining three patients required more than three years of therapy (range: 3.5-7.7 years). For patients who required less than three years of IM therapy for five years of a relapse-free response after the second treatment stop attempt (Fig. 5), a few years of additional IM therapy can reduce the cell population to a small size (e.g., 100~1000 cells). For these patients, we performed additional simulations considering the stochastic behavior of cell populations (Fig. S6 & supplementary methods). Taken together, our simulations confirm that our proposed method can provide a personalized IM therapy duration for a desired TFR$_2$ (e.g., 5-year).

Discussion

This study presents a mathematical model-based approach that can simulate the differentiation dynamics of CML cells during two repeated TFR

attempts. Using longitudinal molecular response measurements and observed clinical outcomes from the TFR$_1$ attempt from a small cohort of 21 patients with chronic myeloid leukemia, we calibrated the model to clinical data and predicted the risk of molecular relapse in TFR$_2$ attempt. By analyzing the relationship between patient-specific model parameters and the TFR$_2$ duration, we were able to identify a binary classifier for the risk of molecular relapse for TFR$_2$ for the patient group: the ratio of the death rate of the leukemic stem cell population to the growth rate of the leukemic progenitor cell population. This classifier separated the low-risk group from the high-risk group in the cohort according to the TFR$_2$ attempt with 76.2% accuracy. A high ratio indicates a higher probability of a sustained TFR$_2$ (i.e., a low risk of relapse) than a low ratio for the cohort of this study since a high value is associated with a faster reduction in the S and P cell populations during IM therapy. Note that the estimated death rate of P cell populations by IM therapy is significantly larger than the growth rate which leads to a reduction of the population during therapy. When IM treatment is stopped, it takes more time for the remaining S and P populations to drive the growth of the D cell population, ultimately reaching the point of molecular relapse.

Several studies have demonstrated that leukemic stem cells (presented in this study as the S cell population) that exist below the current quantitative qRT-PCR detection limit can drive the progression and recurrence of disease [48–50]. Eradicating leukemic stem cells by long-term IM therapy can improve patient outcomes [37,49]. A previous study concluded that the intrinsic turnover property of leukemic stem cells might drive different outcomes (cure vs. non-cure) of an IM stop trial [24]. Therefore, our mathematical model took the S cell population into account to simulate drug responses and revealed that the decay rate of the S cell population (δ_S) in response to IM treatment was one of the critical factors for determining the risk of molecular relapse in the TFR$_2$ attempt. We acknowledge that the effect of IM on leukemic stem cells remains a matter of debate; For example, some argue that leukemic stem cells are refractory to IM [51,52] However, as described in the mathematical modeling section (materials and methods), other studies based on clinical data raised the possibility that IM can reduce leukemic stem cells. Further, our parameterization showed that the average death rate of leukemic stem cells was 0.002 per day (range: 0 ~ 0.01). For some patients ($n = 4$), the estimated average death rate was zero (no leukemic stem cell death by IM). For other patients the death rates were somewhat higher (e.g., > 0.005, $n = 5$). We observed heterogeneous death rates among leukemic stem cell populations by an IM therapy. Notably, the estimated average death rates of leukemic progenitor cells were much higher (0.27 per day) than those of stem cells. These results agree with the opinion that leukemic stem cells may be refractory to IM; however, the death rate of leukemic stem cells should not be ignored for the model to precisely simulate patient responses.

Our study suggests the potential value of model simulations in predicting the optimal IM therapy duration for achieving a sustained TFR$_2$. For each patient predicted to have a low risk of TFR$_2$, an actionable model could be used to predict the optimal IM therapy duration for better clinical outcomes (specifically, a longer TFR$_2$ duration). The predicted optimal therapy duration was highly diverse among patients. Once it is validated with more clinical data, this model is expected to be useful for tailoring IM therapy stop attempts in a clinical context.

This study examined a cohort consisting of a relatively small number of patients (21 patients). A future study involving a more extensive clinical data set would further increase the accuracy of the predictive model. The model developed here is a simplified representation of what may actually be happening in CML under treatment on and off; future studies could also include additional complexities involved in this process. For example, our model could be improved via the integration of additional factors, such as individual immunological factors known to be associated with TFR [53–55]. An additional extension could involve the inclusion of leukemic cells' interactions with normal hematopoietic cells in the model, as these
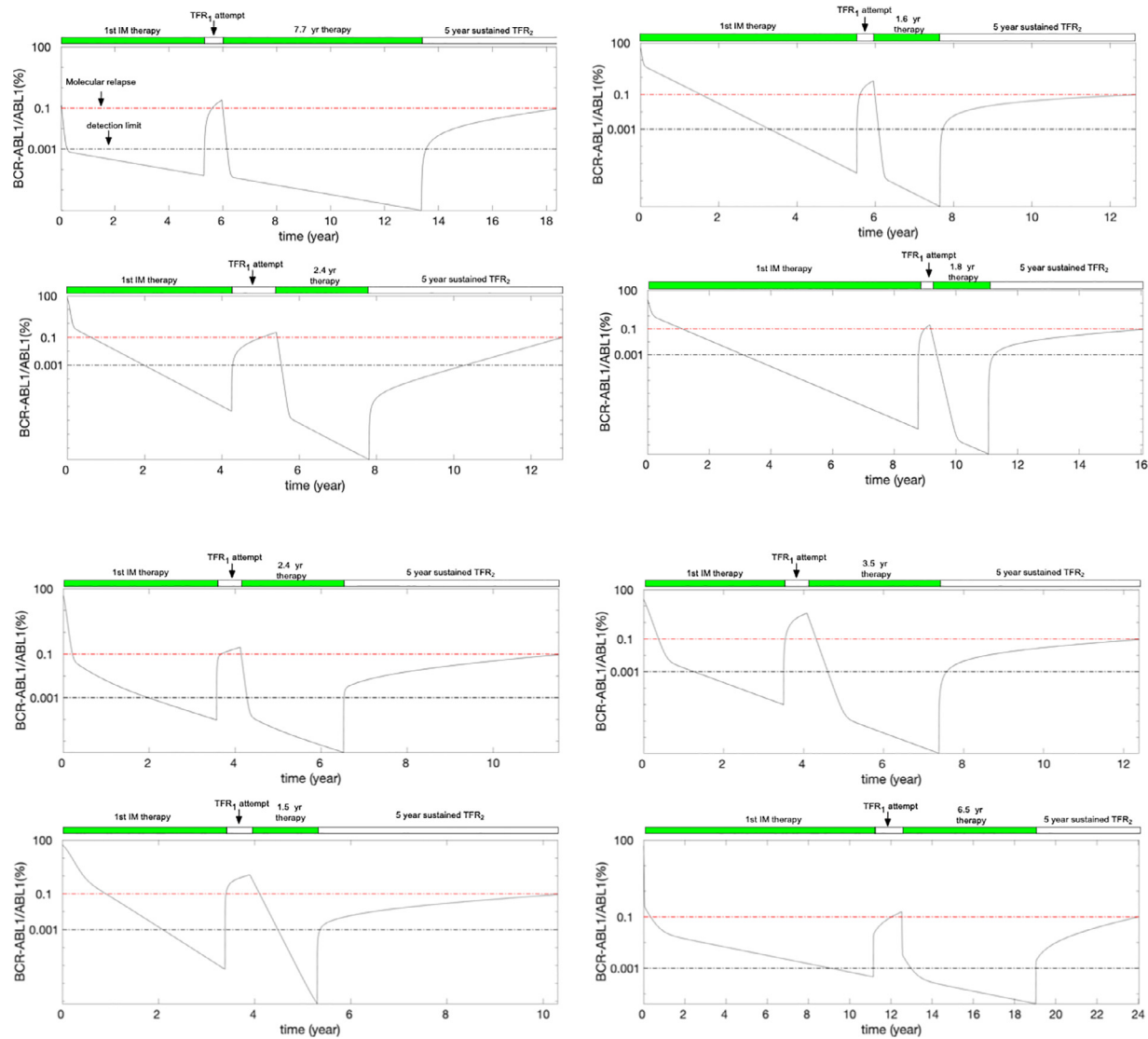
Fig. 5. Optimal treatment duration for the patients in the low-risk group ($n = 8$). The green bar indicates the therapy on period, and the white bar indicates the therapy off period.

interactions could contribute to disease dynamics and treatment resistance. For example, the hematopoietic stem cell migration between the bone marrow and the peripheral blood demonstrated that selective advantage was required for a significant expansion of the cell population to a point large enough to be detected [56]. The competition between normal hematopoietic cells and leukemic cells for bone marrow spaces could modulate disease progression [57]. The cytokine dependency for leukemic cell growth could determine their competitive advantage over normal cells, which could in turn modulate disease progression [58]. The competition mediated by the various types of regulatory feedback that are shared between stem cell and normal cell populations could modulate stem cell expansion [59]. An extended model that considers these additional factors as well as others could be beneficial for suggesting optimal combination therapy or sequential therapy involving kinase inhibitors (e.g., IM) in combination with an immune response modulator (e.g., interferon).

In conclusion, this study demonstrated that a mathematical model based on the biology of the hematopoietic stem cell differentiation system had high predictive power on a retrospective data set of patients with CML ($n = 21$). The integration of this model with longitudinal *BCR-ABL1/ABL1*

data from each patient revealed the underlying cell dynamics that drive *BCR-ABL1/ABL1* transcript changes. Finally, we proposed binary classifier factors that are predictive for the risk of relapse during TFR$_2$. Future studies can further validate the power of this mathematical model by considering more patients as well as more factors. In combination with the Sokal score [60] and ELTS,[61] which are currently used to predict the risk of relapse during an TFR attempt, these mathematical model-based predictive factors could ultimately aid in the accurate selection of low-risk patients for TKI discontinuation.

Declaration of Competing Interest

CRediT authorship contribution statement

Eunjung Kim: Visualization, Formal analysis, Methodology, Writing – original draft. **Eo-Jin Hwang:** Data curation, Writing – review & editing. **Junghye Lee:** Methodology, Writing – review & editing. **Dae-Young Kim:** Methodology, Writing – review & editing. **Jae-Young Kim:** Visualization, Formal analysis, Writing – review & editing. **Dong-Wook Kim:** Visualization, Data curation, Methodology, Writing – review & editing.

Acknowledgments

Supplementary materials

Supplementary material associated with this article can be found, in the online version, at doi:10.1016/j.neo.2022.100817.

References

[1] Hehlmann R, Hochhaus A, Baccarani M, European L. Chronic myeloid leukaemia. *Lancet* 2007;**370**(9584):342–50.

[2] Melo JV, Barnes DJ. Chronic myeloid leukaemia as a model of disease evolution in human cancer. *Nat Rev Cancer* 2007;**7**(6):441–53.

[3] Druker BJ, Guilhot F, O'Brien SG, et al. Five-year follow-up of patients receiving imatinib for chronic myeloid leukemia. *N Engl J Med* 2006;**355**(23):2408–17.

[4] Gambacorti-Passerini C, Antolini L, Mahon FX, et al. Multicenter independent assessment of outcomes in chronic myeloid leukemia patients treated with imatinib. *J Natl Cancer Inst* 2011;**103**(7):553–61.

[5] Kantarjian H, O'Brien S, Jabbour E, et al. Improved survival in chronic myeloid leukemia since the introduction of imatinib therapy: a single-institution historical experience. *Blood* 2012;**119**(9):1981–7.

[6] Branford S, Seymour JF, Grigg A, et al. BCR-ABL messenger RNA levels continue to decline in patients with chronic phase chronic myeloid leukemia treated with imatinib for more than 5 years and approximately half of all first-line treated patients have stable undetectable BCR-ABL using strict sensitivity criteria. *Clin Cancer Res* 2007;**13**(23):7080–5.

[7] de Lavallade H, Apperley JF, Khorashad JS, et al. Imatinib for newly diagnosed patients with chronic myeloid leukemia: incidence of sustained responses in an intention-to-treat analysis. *J Clin Oncol* 2008;**26**(20):3358–63.

[8] Kim D, Goh HG, Kim SH, et al. Comprehensive therapeutic outcomes of frontline imatinib mesylate in newly diagnosed chronic phase chronic myeloid leukemia patients in Korea: feasibility assessment of current ELN recommendation. *Int J Hematol* 2012;**96**(1):47–57.

[9] Caldemeyer L, Dugan M, Edwards J, Akard L. Long-term side effects of tyrosine kinase inhibitors in chronic myeloid leukemia. *Curr Hematol Malig Rep* 2016;**11**(2):71–9.

[10] Hartmann JT, Haap M, Kopp HG, Lipp HP. Tyrosine kinase inhibitors - a review on pharmacology, metabolism and side effects. *Curr Drug Metab* 2009;**10**(5):470–81.

[11] Lee SE, Choi SY, Bang JH, et al. Predictive factors for successful imatinib cessation in chronic myeloid leukemia patients treated with imatinib. *Am J Hematol* 2013;**88**(6):449–54.

[12] Mahon FX, Rea D, Guilhot J, et al. Discontinuation of imatinib in patients with chronic myeloid leukaemia who have maintained complete molecular remission for at least 2 years: the prospective, multicentre Stop Imatinib (STIM) trial. *Lancet Oncol* 2010;**11**(11):1029–35.

[13] Ross DM, Branford S, Seymour JF, et al. Safety and efficacy of imatinib cessation for CML patients with stable undetectable minimal residual disease: results from the TWISTER study. *Blood* 2013;**122**(4):515–22.

[14] Rousselot P, Charbonnier A, Cony-Makhoul P, et al. Loss of major molecular response as a trigger for restarting tyrosine kinase inhibitor therapy in patients with chronic-phase chronic myelogenous leukemia who have stopped imatinib after durable undetectable disease. *J Clin Oncol* 2014;**32**(5):424–30.

[15] Thielen N, van der Holt B, Cornelissen JJ, et al. Imatinib discontinuation in chronic phase myeloid leukaemia patients in sustained complete molecular response: a randomised trial of the Dutch-Belgian Cooperative Trial for Haemato-Oncology (HOVON). *Eur J Cancer* 2013;**49**(15):3242–6.

[16] Takahashi N, Kyo T, Maeda Y, et al. Discontinuation of imatinib in Japanese patients with chronic myeloid leukemia. *Haematologica* 2012;**97**(6):903–6.

[17] Lee SE, Choi SY, Song HY, et al. Imatinib withdrawal syndrome and longer duration of imatinib have a close association with a lower molecular relapse after treatment discontinuation: the KID study. *Haematologica* 2016;**101**(6): 717–723.

[18] Kota V, Atallah E. Musculoskeletal pain in patients with chronic myeloid leukemia after tyrosine kinase inhibitor therapy cessation. *Clin Lymphoma Myeloma Leuk* 2019;**19**(8):480–7.

[19] Daher-Reyes GS, Bence-Bruckler I, Busque L, et al. BCR-ABL1 qPCR-based doubling time within the first 6 months after imatinib discontinuation is a predictive of successful TKI treatment-free remission. *Blood* 2019;**134**(Supplement_1):2933 2933.

[20] Hochhaus A, Baccarani M, Silver RT, et al. European LeukemiaNet 2020 recommendations for treating chronic myeloid leukemia. *Leukemia* 2020;**34**(4):966–84.

[21] Shanmuganathan N, Pagani IS, Ross D M, et al. Early BCR-ABL1 kinetics are predictive of subsequent achievement of treatment-free remission in chronic myeloid leukemia. *Blood* 2020:1196–207. doi:10.1182/blood.2020005514. PMID: 32871588.

[22] Shen N, Liu T, Liu W, et al. A folate receptor 3 SNP promotes mitochondria-induced clonogenicity of CML leukemia cells: Implications for treatment free remission. *Clin Transl Med* 2021;**11**(2):e317.

[23] Michor F, Hughes TP, Iwasa Y, et al. Dynamics of chronic myeloid leukaemia. *Nature* 2005;**435**(7046):1267–70.

[24] Tang M, Foo J, Gonen M, Guilhot J, Mahon FX, Michor F. Selection pressure exerted by imatinib therapy leads to disparate outcomes of imatinib discontinuation trials. *Haematologica* 2012;**97**(10):1553–61.

[25] Horn M, Glauche I, Muller MC, et al. Model-based decision rules reduce the risk of molecular relapse after cessation of tyrosine kinase inhibitor therapy in chronic myeloid leukemia. *Blood* 2013;**121**(2):378–84.

[26] Morrison SJ, Hemmati HD, Wandycz AM, Weissman IL. The purification and characterization of fetal liver hematopoietic stem-cells. *Proc Natl Acad Sci USA* 1995;**92**(22):10302–6.

[27] Morrison SJ, Uchida N, Weissman IL. The biology of hematopoietic stem cells. *Ann Rev Cell Dev Biol* 1995;**11**:35–71.

[28] Riether C, Schurch CM, Ochsenbein AF. Regulation of hematopoietic and leukemic stem cells by the immune system. *Cell Death Differ* 2015;**22**(2):187–98.

[29] Ichimzru M, Ishimaru T, BJ L. Incidence of leukemia in atomic bomb survivors belonging to a fixed cohort in Hiroshima and Nagasaki, 1950–71: radiation dose, years after exposure, age at exposure, and type of leukemia. *J Radiat Res* 1978;**19**(3):262–82.

[30] Martins VC, Busch K, Juraeva D, et al. Cell competition is a tumour suppressor mechanism in the thymus. *Nature* 2014;**509**(7501):465–70.

[31] Ramos CV, Martins VC. Cell competition in hematopoietic cells: quality control in homeostasis and its role in leukemia. *Dev Biol* 2021;**475**:1–9.

[32] Baryawno N, Przybylski D, Kowalczyk MS, et al. A cellular taxonomy of the bone marrow stroma in homeostasis and leukemia. *Cell* 2019;**177**(7):1915–32 e1916.

[33] Duarte D, Hawkins ED, Akinduro O, et al. Inhibition of endosteal vascular niche remodeling rescues hematopoietic stem cell loss in AML. *Cell Stem Cell* 2018;**22**(1):64–77 e66.

[34] Baccarani M, Saglio G, Goldman J, et al. Evolving concepts in the management of chronic myeloid leukemia: recommendations from an expert panel on behalf of the European LeukemiaNet. *Blood* 2006;**108**(6):1809–20.

[35] Roeder I, Horn M, Glauche I, Hochhaus A, Mueller MC, Loeffler M. Dynamic modeling of imatinib-treated chronic myeloid leukemia: functional insights and clinical implications. *Nat Med* 2006;**12**(10):1181–4.

[36] Houshmand M, Blanco TM, Circosta P, et al. Bone marrow microenvironment: the guardian of leukemia stem cells. *World J Stem Cells* 2019;**11**(8):476–90.

[37] Tang M, Gonen M, Quintas-Cardama A, et al. Dynamics of chronic myeloid leukemia response to long-term targeted therapy reveal treatment effects on leukemic stem cells. *Blood* 2011;**118**(6):1622–31.

[38] Tomasetti C. A new hypothesis: imatinib affects leukemic stem cells in the same way it affects all other leukemic cells. *Blood Cancer J* 2011;**1**(5):e19.

[39] Apperley JF. Chronic myeloid leukaemia. *Lancet* 2015;**385**(9976):1447–59.

[40] Fassoni AC, Baldow C, Roeder I, Glauche I. Reduced tyrosine kinase inhibitor dose is predicted to be as effective as standard dose in chronic myeloid leukemia: a simulation study based on phase III trial data. *Haematologica* 2018;**103**(11):1825–34.

[41] Rosti G, Castagnetti F, Gugliotta G, Baccarani M. Tyrosine kinase inhibitors in chronic myeloid leukaemia: which, when, for whom? *Nat Rev Clin Oncol* 2017;**14**(3):141–54.

[42] Elmaagacli AH, Freist A, Hahn M, et al. Estimating the relapse stage in chronic myeloid leukaemia patients after allogeneic stem cell transplantation by the amount of BCR-ABL fusion transcripts detected using a new real-time polymerase chain reaction method. *Br J Haematol* 2001;**113**(4):1072–5.

[43] Hochhaus A, Lin F, Reiter A, et al. Quantification of residual disease in chronic myelogenous leukemia patients on interferon-alpha therapy by competitive polymerase chain reaction. *Blood* 1996;**87**(4):1549–55.

[44] Kantarjian HM, Talpaz M, Cortes J, et al. Quantitative polymerase chain reaction monitoring of BCR-ABL during therapy with imatinib mesylate (STI571; gleevec) in chronic-phase chronic myeloid leukemia. *Clin Cancer Res* 2003;**9**(1):160–6.

[45] Loh WY. Regression trees with unbiased variable selection and interaction detection. *Stat Sin* 2002;**12**:361–86 2002.

[46] Loh WY, Shih YS. Split selection methods for classification trees. *Stat Sin* 1997;**7**:815–40.

[47] Fawcett T. An introduction to ROC analysis. *Pattern Recognit Lett* 2006;**27**(8):861–74.

[48] Wilson A, Laurenti E, Oser G, et al. Hematopoietic stem cells reversibly switch from dormancy to self-renewal during homeostasis and repair. *Cell* 2008;**135**(6):1118–29.

[49] Stein AM, Bottino D, Modur V, et al. BCR-ABL transcript dynamics support the hypothesis that leukemic stem cells are reduced during imatinib treatment. *Clin Cancer Res* 2011;**17**(21):6812–21.

[50] Essers MA, Trumpp A. Targeting leukemic stem cells by breaking their dormancy. *Mol Oncol* 2010;**4**(5):443–50.

[51] Houshmand M, Simonetti G, Circosta P, et al. Chronic myeloid leukemia stem cells. *Leukemia* 2019;**33**(7):1543–56.

[52] Reynaud D, Pietras E, Barry-Holson K, et al. IL-6 controls leukemic multipotent progenitor cell fate and contributes to chronic myelogenous leukemia development. *Cancer Cell* 2011;**20**(5):661–73.

[53] Burchert A, Saussele S, Eigendorff E, et al. Interferon alpha 2 maintenance therapy may enable high rates of treatment discontinuation in chronic myeloid leukemia. *Leukemia* 2015;**29**(6):1331–5.

[54] Hahnel T, Baldow C, Guilhot J, et al. Model-based inference and classification of immunologic control mechanisms from TKI cessation and dose reduction in patients with CML. *Cancer Res* 2020:2394–406. doi:10.1158/0008-5472.CAN-19-2175. Epub 2020 Feb 10. PMID: 32041835.

[55] Ilander MM, Olsson-Stromberg U, Lahteenmaki H, et al. Disease relapse after TKI discontinuation in CML is related both to low number and impaired function of NK-cells:data from Euro-SKI. *Blood* 2013;**122**(21).

[56] Ashcroft P, Manz MG, Bonhoeffer S. Clonal dominance and transplantation dynamics in hematopoietic stem cell compartments. *PLoS Comput Biol* 2017;**13**(10):e1005803.

[57] Stiehl T, Wang W, Lutz C, Marciniak-Czochra A. Mathematical modeling provides evidence for niche competition in human AML and serves as a tool to improve risk stratification. *Cancer Res* 2020;**80**(18):3983–92.

[58] Stiehl T, Ho AD, Marciniak-Czochra A. Mathematical modeling of the impact of cytokine response of acute myeloid leukemia cells on patient prognosis. *Sci Rep* 2018;**8**(1):2809.

[59] Weiss LD, van den Driessche P, Lowengrub JS, Wodarz D, Komarova NL. Effect of feedback regulation on stem cell fractions in tissues and tumors: Understanding chemoresistance in cancer. *J Theor Biol* 2021;**509**:110499.

[60] Sokal JE, Cox EB, Baccarani M, et al. Prognostic discrimination in "good-risk" chronic granulocytic leukemia. *Blood* 1984;**63**(4):789–99.

[61] Pfirrmann M, Clark RE, Prejzner W, et al. The EUTOS long-term survival (ELTS) score is superior to the Sokal score for predicting survival in chronic myeloid leukemia. *Leukemia* 2020;**34**(8):2138–49.